PNAS
www.pnas.org

Supplementary Information for

Physical limits of flight performance in the heaviest soaring bird

Williams, H.J.†, Shepard, E.L.C.†*, Holton, M.D., Alarcón, P.A.E., Wilson, R.P. & Lambertucci, S.A.

*Corresponding author: e.l.c.shepard@swansea.ac.uk

† Indicates joint first authorship

This PDF file includes:

Supplementary text
Figures S1 to S8
Tables S1 to S3
SI References

Supplementary text

Tag deployment

Data were collected in Northwest Patagonia, where the topography ranges from the high Andes (≤ 4,000 m above sea level [ASL]) to the flatter steppe (*ca*. 800 m ASL) (see (1)). We trapped 24 Andean condors and selected 8 immature birds (from 2-6 years old, age classes were separated using feather characteristics and beak colour and estimated to the nearest 6 months (2)) to be equipped with loggers in the Austral summers of 2013, 2014 and 2018 as described in Lambertucci *et al*. (3). Immature birds were selected as their use of roosts in the steppe increased the likelihood of locating the archival tags after remote drop-off. The archival unit included an iGotU-GPS logger (Mobile Action Technology, model GT-120) and a Daily Diary (hereafter, DD; Wildbyte Technologies; (4)), which included the following: A tri-axial accelerometer (*g*; gravitational acceleration), tri-axial magnetometer (gauss), barometric pressure sensor (mbar) and temperature sensor (degrees). DDs were programmed to sample acceleration at either 20 or 40 Hz and other parameters at lower frequencies (2-13 Hz). The GPS logger was programmed to record one location per minute and was packaged with the DD in a 3-d printed housing. The complete DD-GPS package had a mass of 0.093 kg (representing ~1% of bird body mass), dimensions of 65 x 56 x 26 mm, and was attached to the lower back using black Tesa Tape. The high volume of data recorded required us to retrieve the loggers. The package was designed to detach at a predetermined time, using an automated release mechanism based on the heating of nichrome wire that was looped through a stretch of fishing line. The released package was located using the last recorded position from the GPS-GSM data prior to drop-off (programmed to record locations every 15 min (3)) and a miniature VHF transmitter within the housing. DD data were processed as described below using the custom-built software DDMT (Wildbytes, http://wildbytetechnologies.com/research.html). All data are available on Movebank (within the study: Andean Condor (*Vultur gryphus*), Immatures, Bariloche, Argentina, 2013-2018 https://www.movebank.org/cms/webapp?gwt_fragment=page=studies,path=study1109284853).

Data processing

Movement data

We assessed the amount of flapping undertaken in all flights, but selected flights over 10 minutes for further analyses, as these were most likely to represent departures from roost or foraging sites. Flight effort was assessed using a single metric derived from the acceleration data that quantifies body motion, increasing with both the frequency and amplitude of the flapping signal: Vectorial Dynamic Body Acceleration (VeDBA) (5). This was derived by smoothing the raw acceleration data with a running mean over two complete flapping cycles to derive the gravitational component, which was subtracted from the raw data in each of the three acceleration channels (6). VeDBA values were then further

smoothed to produce a consistent activity threshold from which flapping (smoothed VeDBA > 0.5 *g*) and non-flapping flight (smoothed VeDBA < 0.5 *g*) were classified.

Take-off periods were labelled for each flight. These periods began when a bird left the ground, identifiable from the barometric pressure, and continued until flapping ceased for ≥ 15 seconds (Fig. S1). The total VeDBA during take-off was taken as a measure of take-off effort, which increased with the amplitude and frequency of the dynamic movements as well as take-off duration.

We used Boolean-based classification algorithms (7) to identify and label flight behaviours (Table S1), which were defined (from non-flapping flight) as follows: Gliding (a sustained loss of altitude), thermal soaring (sustained increase in altitude with continuous rotation in heading, evident in the magnetometry data) and slope soaring (sustained maintenance or increase in altitude without rotation) (see (8, 9)). The main potential case for misidentification would be if birds soared along thermal streets, exploiting thermals by flying without turning, however, inspection of a subset of dead-reckoned tracks (see (10)) suggested most slope soaring behaviour occurred along slopes, suggesting misclassification did not happen frequently. Climb-glide cycles were then categorised by updraft type, resulting in glides being classified as inter-thermal glides (hereafter, ITGs; thermal-to-thermal) and inter-slope glides (hereafter, ISGs; slope-to-slope), with glides remaining unclassified if they occurred between different lift types. In order to assess the distribution of flight effort within classified glides, data were summarised into 1 second bins and glides were categorised as containing flapping when they included a minimum of one bin with flapping flight. The statistical framework used here is consistent with that of previous bio-logging work, although the approach of classifying behaviour prior to the use of statistical models to relate this behaviour to environmental variables may be overly precise (given error is reduced with this two-level approach, with the use of Boolean-based classification followed by statistical analyses).

A binary variable was created to categorise whether flights occurred before or after feeding (and therefore when birds were lighter or heavier). This was done by classifying landing periods as either active or non-active, where a dramatic increase in the activity levels of the bird on the ground indicated feeding or social interaction (Fig. S2), with the two behaviours being highly correlated (Additional support for using this method is provided in (11)).

Environmental parameters

Hourly values of wind speed (km h^{-1}) were taken from Bariloche airport weather station (accessed at Weather Underground, https://www.wunderground.com/). Altitude above sea level (ASL) and vertical velocity (m s^{-1}) in flight were derived from the on-board barometric pressure sensor. Pressure values were smoothed using a running mean over 10 seconds (8) and converted to altitude using hourly records of sea-level pressure from Bariloche weather station. Altitude ASL was used in models of flight effort

as continuous data were available for all flight and effort data. The effect of topography on overall flight effort was assessed in terms of longitude, which is correlated with a shift from the relatively flat steppe, to the mountainous Andes (moving East to West) (1).

Altitude above sea level was also used in the analysis of effort within glides, as many glides were without a GPS fix, precluding the use of altitude above ground (AGL). Where GPS fixes were available, they occurred within 10 to 60 s of the end of the glide. This, combined with the resolution of the topographic data (30 m), the cross country speed of birds, and the changing slope of the terrain, meant that error in the estimation of height above ground at the end of the glides would be difficult to quantify to a high degree of accuracy, for the majority of glides (12). Nonetheless, our assumption that the altitude above ground level decreases within glides (as well as above sea level) is supported by the data available for the small number of glides (n = 29) with more than 3 GPS fixes (Fig. S7).

Statistical analyses

A series of analyses was performed to examine predictors of flight effort at a range of spatiotemporal scales. At the broadest scale we assessed variation in effort across all travelling flights. We then examined the specific circumstances associated with increased flight effort during glides between updrafts.

Effort in travelling flight and take-off

We used a linear mixed effects model (LMM) to assess predictors of overall flight effort (mean VeDBA per 10 second window, transformed by log10). The global model included the fixed effects of mean altitude (centred and scaled) in interaction with flight type (a three-level factor: non-flapping flight, flapping and take-off) and wind speed (centred and scaled), also in interaction with flight type. As flight height and wind speed were related to time of day (and therefore thermal strength), thermal strength was not included as a separate variable. Condor ID was included as a random effect. Given that flapping was relatively rare, the total sample size (N = 8776, 10 second sections) included a random sample of non-flapping flight, to equal the number of flapping and take-off samples (non-flapping = 4388, take-off = 864, flapping = 3524).

Flight effort is also likely to vary before or after feeding. Rather than include an additional interaction between flight type, feeding activity and wind in the global model, we used a Kruskal-Wallis test to quantify the difference in total take-off effort (total VeDBA) following active and non-active periods on the ground. Finally, we expected flight effort to be lower in the Andes than the steppe due to the increased slope angle on the production of both thermal and orographic updrafts. The effect of topography on flight effort was quantified in a second LMM with a reduced dataset representing instances where effort data (summarised in 10 second windows) were associated with GPS locations.

Here, flight effort (mean VeDBA) was modelled as a function of longitude (see above) and wind speed, both in interaction with flight type, as well as the random effect of condor ID.

Effort in gliding between updrafts

We then assessed whether the use of flapping flight varied with the type of updraft that birds were moving between (thermal or slope lift). Here, we used a Chi-squared test to compare the proportion of glides where flapping occurred and a Kruskal Wallis chi-squared test to compare the amount of flapping when used. We then examined whether flapping was more likely to occur at a specific point through the glide or if distributed evenly. The timing of flapping was defined in terms of the proportion of time through the glide when "flapping bins" occurred. The median occurrence of flapping was then compared to a random distribution of flapping using a paired t-test, performed for all ITGs and again for ISGs. Tests were bootstrapped with 1000 repeats and the mean p-value ($\bar{x}$p) for each glide type across these repeats.

Finally, we tested whether birds flap more when moving between thermals that are weak or when operating in windy conditions. Specifically, we used t-tests to assess whether the occurrence of flapping (in the ITG as a binary presence or absence response) was predicted by i) the climb rate of the bird in the previous thermal, or ii) the wind speed. This dataset was restricted to glides that immediately followed a thermal climb, with no break in flight classification. We also tested whether the number of flapping events was related to the previous thermal climb rate, taking only those glides where flapping was present, and testing this with a Spearman's rank correlation.

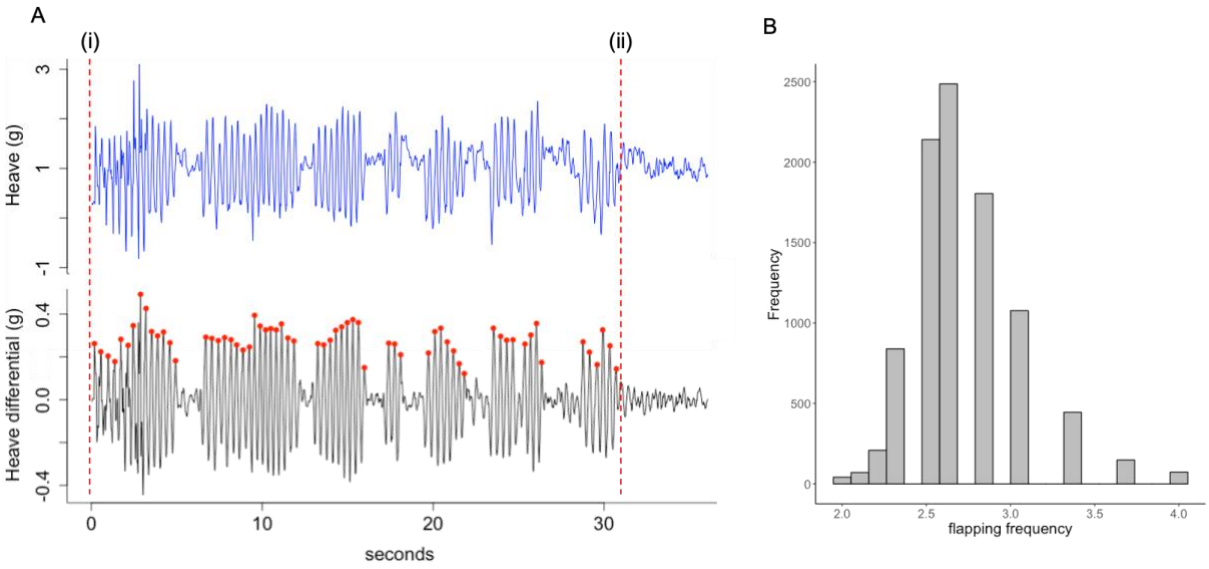

Fig. S1. Classification of the take-off period and flapping frequency. (A) Take-off was labelled from the moment that the bird became airborne, as indicated by the pressure change that was usually associated with a burst of flapping (i), until flapping ceased (ii). Flapping occurred in bouts (each flap is indicated by a peak in the heave differential, red points) and take-off ended when there was no more flapping within 15 seconds of the previous bout. The wingbeat signal varied in amplitude, with greater variation in amplitude in the first one or two seconds of take-off (B) Wingbeat frequencies averaged ~2.7 beats per second. Only 40 Hz data were used to describe the flapping frequencies.

Table S1. Flexible time algorithms in a Boolean approach for classification of flight periods. The series of base elements applied for the classification of gliding, soaring and thermal soaring flight periods. Each base element has a defined temporal flexibility that includes a number of events over which the conditions of the element are met, as well as a range to the next element, a window of flexibility and a period over which the element is extended (ETNE, where the units are in events, 40 Hz having 40 events per second). See Wilson et al. (7) for details of use of these algorithms in the Boolean approach. Values given were used for 20 Hz data and doubled for 40 Hz data.

GLIDING	BE	PRESENT	RANGE	FLEXIBILITY	ETNE
TS1	Glide	200	201	10000	201
TS2	Soar	20			

SOARING	BE	PRESENT	RANGE	FLEXIBILITY	ETNE
TS1	Soar	200	201	10000	201
TS2	Glide	20			

THERMAL SOARING	BE	PRESENT	RANGE	FLEXIBILITY	ETNE
TS1	Soar	20	21	2000	1
TS2	Turn 1	25	40	250	
TS3	Turn 2	25	40	250	
TS4	Turn 1	25	40	250	
TS5	Turn2	25	26	25	
TS6	Soar	20	21	10000	500
TS7	Glide	20			

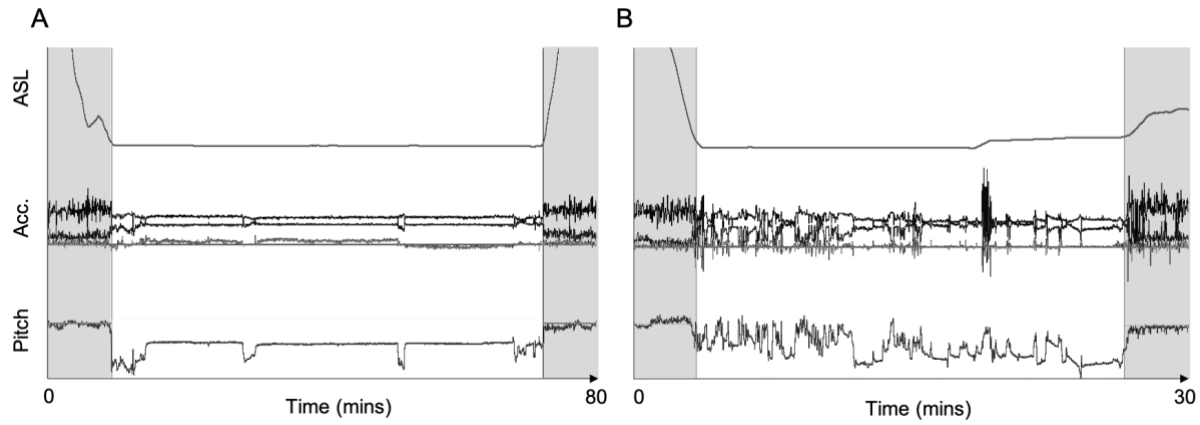

Fig. S2. Classification of foraging behaviour. Time series data showing changes in body activity (raw tri-axial acceleration, "Acc.") and body pitch corresponding to A) non-active and B) active landing periods. Flight periods are shown in grey bands and periods on the ground in the white sections. It is highly probable that activity on the ground is indicative of feeding behaviour, where low frequency changes in pitch are associated with repeated bending to the carcass, and high frequency changes in raw acceleration with pulling at the carcass and social activity around the carcass (see (11)). Note that flight periods following activity on the ground (B) involve a greater amount of flapping (high frequency variation in the raw acceleration) than take-offs following non-active landing periods (A).

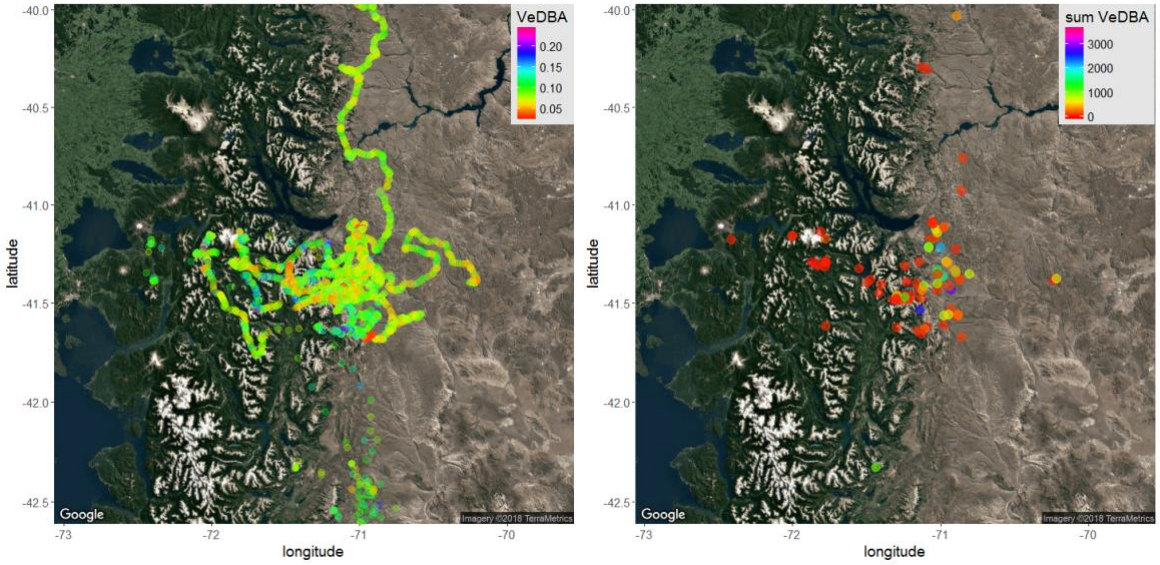

Fig. S3. Spatial patterns in flight effort. Birds concentrate their flight activity over an area of the steppe (in the East of the map) with high concentrations of domestic livestock. Forays into the Andes represent movement to/from roost or nest sites. A) Mean flight effort (mean VeDBA) is shown for each 10 second period with an associated GPS position in travelling flight for all condors. B) Take-off events are coloured by the total effort (VeDBA) required to take off, which will increase with duration, number of flaps or amplitude of the acceleration signal within each flap.

Table S2. Individual variation in flight behaviour. The proportion of flight classified as non-travelling and travelling-flight. For the 6 condors where travelling flight types could be further sub-classified, 32.5% of travelling-flight time was spent in thermal soaring, 12.1% in slope soaring, 46.3 % gliding and 1.2% flapping (the remaining 8% of flight was unclassified), with an average of 27.48 hours of flight per individual (for these 6 birds). Vertical velocity (V_z m s^{-1}) is reported as the median vertical velocity when the bird is climbing in the respective updraft types (i.e. $V_z > 0$) and losing altitude in gliding (i.e. $V_z < 0$) (from 10 second smoothed pressure). The modal hour is the time of the day when use of this updraft type is most frequent for that bird. Note that for condors 1 and 2 flight data could not be categorised as soaring or gliding, but with the combined flapping events, 0.8% of travelling-flight was spent flapping (N = 8 birds).

		Flight times				**Travelling flight types**							
		Short flights		**Travelling flights**		**Thermal soaring**			**Slope soaring**			**Gliding**	
ID	Flapping freq. s^{-1}	Total (hrs)	Total flapping (mins)	Total (hrs)	Total flapping (mins)	hours	V_z (m s^{-1})	Modal hour	hours	V_z (m s^{-1})	Modal hour	hours	V_z (m s^{-1})
9	2.67	0.89	4.10	15.26	6.68	5.16	2.35	14	1.55	1.74	16	7.36	-3.01
33	2.50	1.89	7.35	45.38	39.67	13.43	1.48	12	6.12	1.42	14	21.67	-1.41
58	2.67	3.01	25.33	28.91	27.85	9.28	2.02	13	4.06	1.44	13	12.94	-2.77
60	2.67	2.15	10.96	25.78	16.28	9.44	1.21	12	2.65	1.13	14	11.47	-1.30
61	2.86	3.39	14.27	18.59	8.07	6.83	1.29	14	1.37	1.23	13	8.44	-1.30
62	2.67	2.30	8.71	30.94	16.77	9.41	1.69	11	4.23	1.98	15	14.39	-2.57
1	-	2.69	13.52	28.62	30.91	-	-	-	-	-	-	-	-
2	-	2.47	9.27	23.18	14.46	-	-	-	-	-	-	-	-
$\bar{x}$	2.67 ± 0.36	2.35 ± 0.76	11.69 ± 6.41	27.08 ± 9.14	20.08 ± 11.60	8.93 ± 2.81	1.67 ± 0.44	13	3.33 ±1.82	1.49 ± 0.32	14	12.71 ± 5.13	-2.06 ± 0.81

Table S3. Modelling the effect of altitude, wind and flight type on flight effort. Model output for the GLMM predicting variance in the total effort (VeDBA (*g*)) due to wind speed, altitude and flight type (Intercept 1 = non-flapping flight, flight type 2 = take-off, flight type 3 = flapping in travelling flight). Total effort (sum VeDBA) was calculated over 10 second windows. Wind speed and altitude were averaged over the 10 second window, centred and scaled. The model also included a random effect of condor ID.

Variable	**Est.**	**Std. error**	**t-value**	**ANOVA**		
				X^2	**df**	**P**
Intercept	-0.50	0.05	-42.68			
Altitude	-0.01	0.005	-2.69			
Wind speed	0.04	0.004	10.77	115.3	9,1	<0.001
Flight type 2	1.27	0.02	73.14			
Flight type 3	0.98	0.01	112.38			
Altitude : flight type 2	-0.09	0.01	-4.80			
Altitude : flight type 3	-0.04	0.01	-4.58	37.104	9,2	<0.001

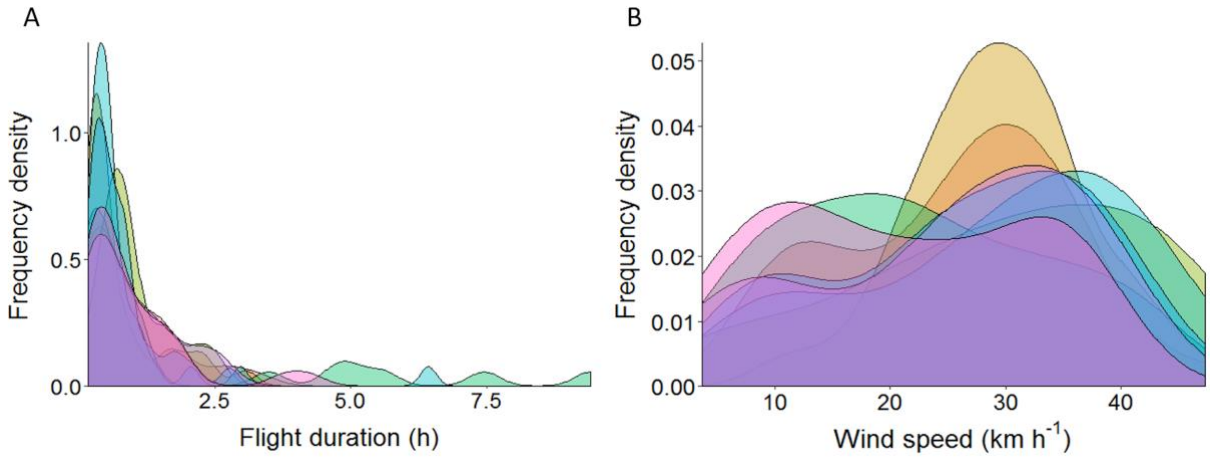

Fig. S4. Flight durations and associated wind speeds, (A) Travelling flight durations per individual (226 flights; median duration = 32 min., N = 8 condors, indicated by colour). (B) Distribution of wind speeds during travelling flights (median = 28 km h^{-1}).

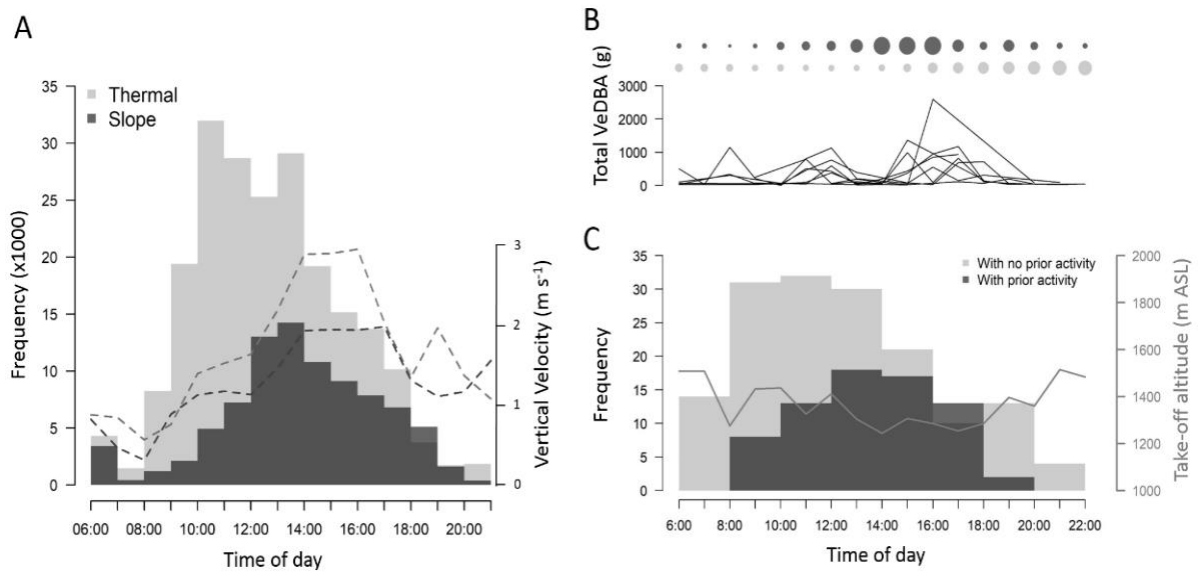

Fig. S5. Daily patterns in flight effort (A) Time spent thermal soaring (light grey) and slope soaring (dark grey) through the day for the 6 condors (N = 271, 264 10-second bins). Soaring behaviour is shown in relation to the mean vertical velocity (V_z m s^{-1}) achieved through the day for thermal soaring (light grey dashed line) and slope soaring (light grey dashed line). The mean V_z is calculated from the positive climb rates. (B) Take-off effort (total VeDBA) through the day for 8 condors. Variation in effort is shown in relation to the daily trends in relative thermal intensity (positive climb rates gained in soaring, grey circles) and relative wind speed (dark circles). (C) Frequency density of foraging (dark grey) and non-active (light grey) landing periods. Take-off after landing to forage occurs later in the day, peaking ~2 pm. Mean altitude at take-off (m above sea level [ASL], black line) decreases through the day as birds land in the steppe to forage and in the mountains in the evening to roost.

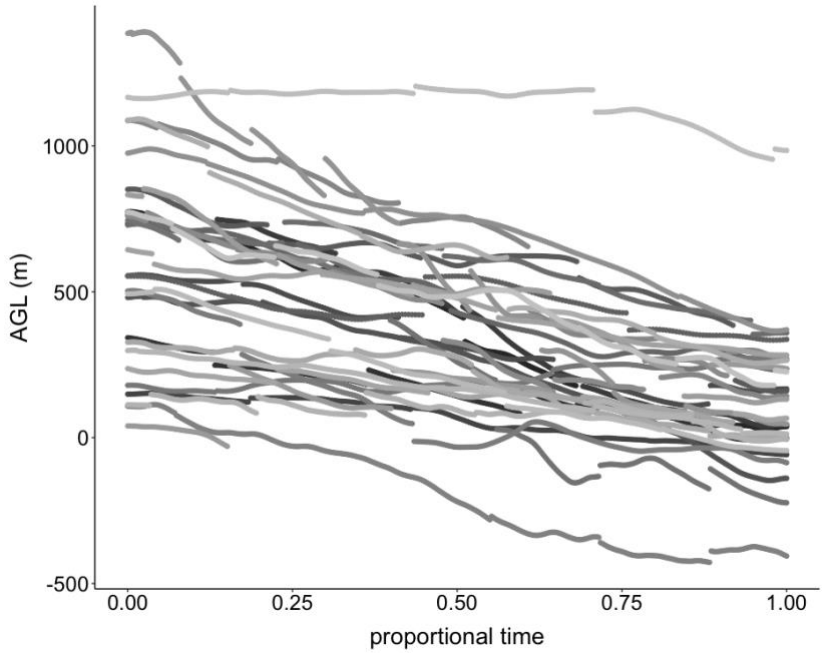

Fig. S6. Altitude above ground level (AGL) decreases through the inter-thermal glides for cases with at least 4 GPS points per glide (i.e. > 3 minute glide duration, N = 29 of 489). Altitude AGL is calculated as the difference between altitude ASL (40 Hz) and the underlying topography (taken at the nearest GPS point within 60 seconds). The mean altitude at the end of these glides is 130 m AGL. However, height estimates AGL could be out by as much as 1254 m (ignoring the 30 m resolution of the DEM) in the case of (i) a 60 second delay between GPS and DD datapoints, resulting in an estimated distance of 814 m between them (taking the mean glide groundspeed of 13.56 m s^{-1}) and (ii) the maximum slope angle in the steppe of 56 ° (mean slope angle = 8 °).

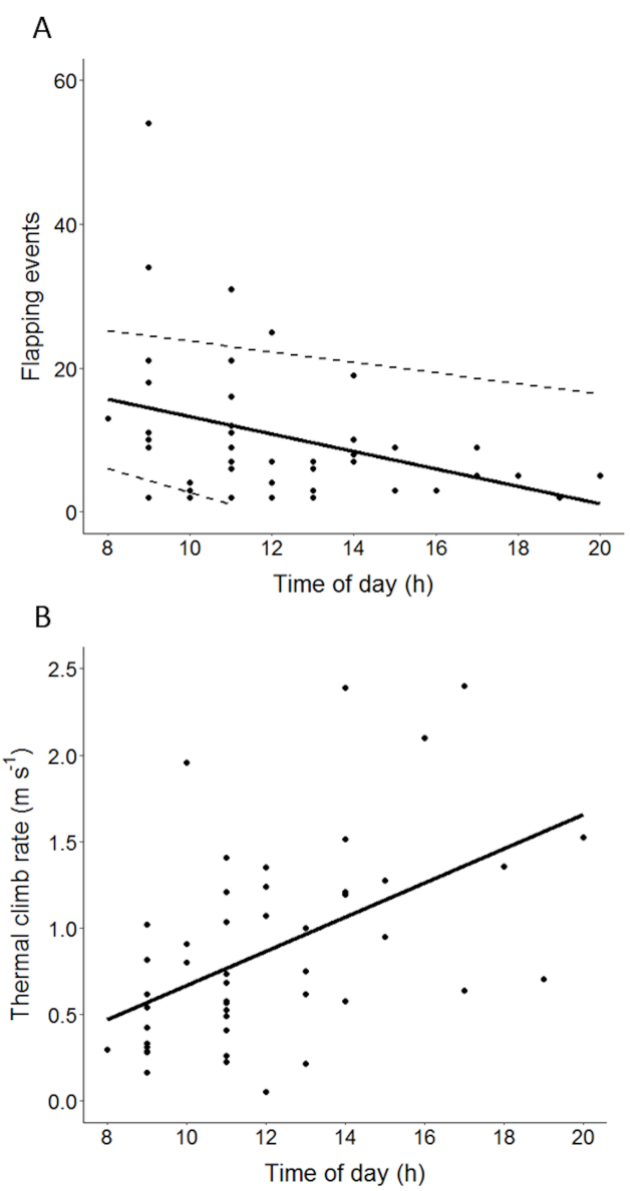

Fig S7. Daily trends in flight parameters. (A) The number of seconds spent flapping in inter-thermal glides (N = 47) decreased through the day (GLM: Est = -1.21, t = -2.566, p = 0.014). (B) Climb rates within thermal updrafts increased through the day ($p<0.001$, $r = 0.526$, Spearman's).

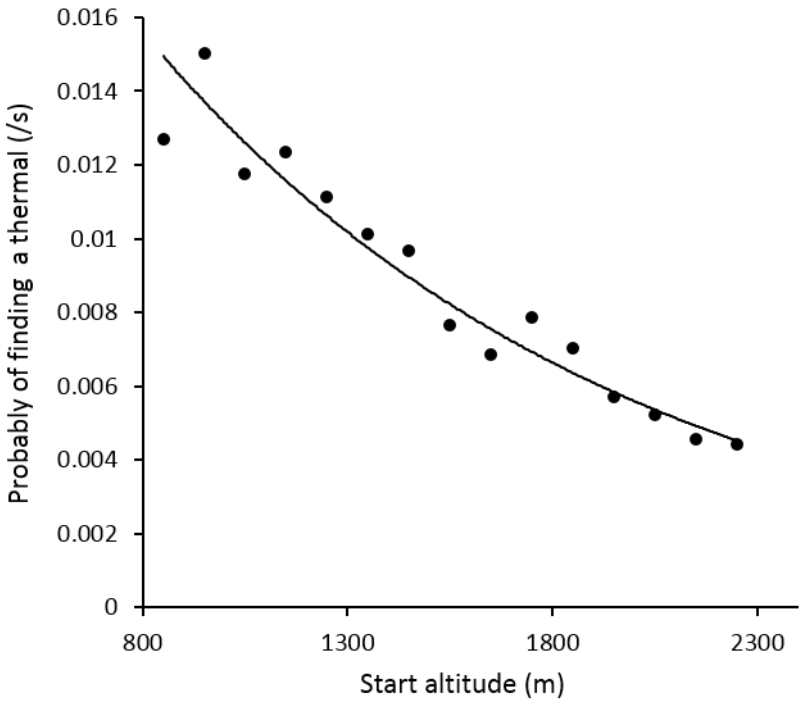

Fig. S8. The probability of entering a new thermal when gliding between thermals. Percentage probability per unit time as a function of start altitude (m above sea level). This is derived as a function of time (ITG duration) using probability theory as described in Wilson *et al.* (13); analogous to search time for foraging birds locating a patch. This negative exponential function reflects the fact that birds leaving a thermal at appreciable height are unlikely to enter another thermal without having travelled appreciably and will therefore glide for longer. Indeed, there are potential disadvantages to entering a thermal when high up, as birds are both travelling and searching for food, the former optimised with increased glide periods where ground speed is greater, and the latter requires them to be reasonably close to the substrate. Nonetheless, the outcome is that the rates at which birds enter new thermals gives us the rate at which they encounter thermals that they deem to be usable/useful. From this we calculated the overall probability (P_T) for finding and using a thermal during the glide (Fig. 4; $P_T = (1\text{-}P_t)_n$; where P_t is the probability of finding a thermal per unit time and n is the number of seconds a bird searches for a thermal).

References:

1. S. A. Lambertucci, *et al.*, Tracking data and retrospective analyses of diet reveal the consequences of loss of marine subsidies for an obligate scavenger, the Andean condor. *Proc. R. Soc. B* **285** (2018).

2. J. del Hoyo, A. Elliott, J. Sargatal, *Handbook of the Birds of the World, Volume 2. New World Vultures to Guineafowl* (Lynx Edicions, 1994).

3. S. A. Lambertucci, *et al.*, Apex scavenger movements call for transboundary conservation policies. *Biol. Conserv.* **170**, 145–150 (2014).

4. R. P. Wilson, E. L. C. Shepard, N. Liebsch, Prying into the intimate details of animal lives: Use of a daily diary on animals. *Endanger. Species Res.* **4**, 123–137 (2008).

5. R. P. Wilson, *et al.*, Estimates for energy expenditure in free-living animals using acceleration proxies: A reappraisal. *J. Anim. Ecol.* **89**, 161-172 (2020).

6. E. L. C. Shepard, *et al.*, Derivation of body motion via appropriate smoothing of acceleration data. *Aquat. Biol.* **4**, 235–241 (2008).

7. R. P. Wilson, *et al.*, Give the machine a hand: A Boolean time-based decision-tree template for rapidly finding animal behaviours in multisensor data. *Methods Ecol. Evol.* **9**, 2206–2215 (2018).

8. H. J. Williams, E. L. C. Shepard, O. Duriez, S. A. Lambertucci, Can accelerometry be used to distinguish between flight types in soaring birds? *Anim. Biotelemetry* **3** (2015).

9. G. Bohrer, *et al.*, Estimating updraft velocity components over large spatial scales: contrasting migration strategies of golden eagles and turkey vultures. *Ecol. Lett.* **15**, 96–103 (2012).

10. O. Bidder, *et al.*, Step by step: reconstruction of terrestrial animal movement paths by dead-reckoning. *Mov. Ecol.* **3**, 1–16 (2015).

11. R. Nathan, *et al.*, Using tri-axial acceleration data to identify behavioral modes of free-ranging animals: general concepts and tools illustrated for griffon vultures. *J. Exp. Biol.* **215**, 986–96 (2012).

12. G. Péron, *et al.*, The challenges of estimating the distribution of flight heights from telemetry or altimetry data. *Anim. Biotelemetry* **8**, 1–13 (2020).

13. R. P. Wilson, *et al.*, Luck in Food Finding Affects Individual Performance and Population Trajectories. *Curr. Biol.* **28**, 3871-3877 (2018).